Bioconjugate Chemistry

Article

pubs.acs.org/bc

Quantum-Dot-Conjugated Graphene as a Probe for Simultaneous Cancer-Targeted Fluorescent Imaging, Tracking, and Monitoring Drug Delivery

Mei-Ling Chen, Ye-Ju He, Xu-Wei Chen, and Jian-Hua Wang*

Research Center for Analytical Sciences, Box 332, Northeastern University, Shenyang 110819, China

Supporting Information

ABSTRACT: We report a novel quantum-dot-conjugated graphene, i.e., hybrid SiO_2-coated quantum dots (HQDs)-conjugated graphene, for targeted cancer fluorescent imaging, tracking, and monitoring drug delivery, as well as cancer therapy. The hybrid SiO_2 shells on the surface of QDs not only mitigate its toxicity, but also protect its fluorescence from being quenched by graphene. By functionalizing the surface of HQDs-conjugated graphene (graphene-HQDs) with transferrin (Trf), we developed a targeted imaging system capable of differential uptake and imaging of cancer cells that express the Trf receptor. The widely used fluorescent antineoplastic anthracycline drug, doxorubicin (DOX), is adsorbed on the surface of graphene and results in a large loading capacity of 1.4 mg mg^{-1}. It is advantageous that the new delivery system exhibits different fluorescence color in between graphene-HQDs and DOX in the aqueous core upon excitation at a same wavelength for the purpose of tracking and monitoring drug delivery. This simple multifunctional nanoparticle system can deliver DOX to the targeted cancer cells and enable us to localize the graphene-HQDs and monitor intracellular DOX release. The specificity and safety of the nanoparticle conjugate for cancer imaging, monitoring, and therapy has been demonstrated in vitro.

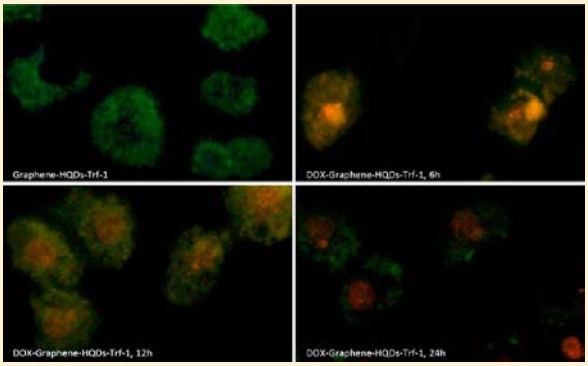

INTRODUCTION

Recently, functionalized graphene nanosystem has been paid extensive attention because of their multifunctional properties, such as larger surface area,[1] lower toxicity,[2] and good stability. Graphene can be used as nanodrug by itself in certain circumstances.[3] Thus, it is believed to have great potential applications in the fields of drug delivery, diagnosis, therapy, and sensing,[2,4] especially in a controlled drug delivery system due to its super capability for loading drug[5] and maintaining a constant rate for drug release. While the functionalized graphene nanosystems of drug delivery represent an exciting advance in the field of nanomedicine, it is ideal to engineer "smart" multifunctional luminescence-functionalized graphene nanosystems that are able to perform the above tasks and at the same time enable visual monitoring of the drug delivery process, e.g., localizing the nanocarrier, tracking the drug, and evaluating the efficiency of drug release.

However, the preparation of luminescence-functionalized graphene is not an easy task because of the zero-bandgap in graphene[6,7] and its nature on fluorescence quenching.[8] Thus, it is highly unlikely to observe photoluminescence (PL) from graphene. In this sense, intensive emission with tunable wavelength of graphene can only be provided by combination with luminescent materials. Quantum dots have been increasingly utilized as biological imaging and labeling probes because of their unique optical properties,[9,10] including broad absorption with narrow photoluminescence spectra, high quantum yield, low photobleaching, and resistance to chemical degradation in comparison with other classical fluorophores. However, the fluorescence of pure QDs is quenched by graphene[11] and the toxicity of cadmium or tellurium is a problem.[12] Considering the complicate intracellular conditions, the luminescence material in the functionalized graphene nanosystems should have good pH stability and high PL efficiency, and are less sensitive to the surrounding chemicals, in order to achieve visual monitoring of the process of drug delivery and localizing the nanocarrier. The silica-coated QDs (HQDs) have a hybrid structure by forming CdS-like clusters in the vicinity of CdTe nanocrystals in the SiO_2 shells, showing a drastic increase in PL efficiency with respect to pure CdTe nanocrystals.[13] The hybrid SiO_2 shells on the surface of QDs, which are chemically inactive and biocompatible,[14] will serve a dual function as a cover layer to mitigate the toxicity of QDs and protect the fluorescence of QDs from being quenched by graphene.

In the present study, we report a novel design of a nanoassembly by capping graphene surfaces with HQDs via a simple electrostatic layer-by-layer assembly protocol (Scheme 1). The material is further advanced by tailoring its surface with Trf ligands for targeted recognition of cancer cells.[15,16]

Received: August 29, 2012
Revised: January 29, 2013
Published: February 21, 2013

   dx.doi.org/10.1021/bc3004809 | *Bioconjugate Chem.* 2013, 24, 387−397

Scheme 1. Preparation of Water Dispersible DOX-Graphene-HQDs-Trf[a]

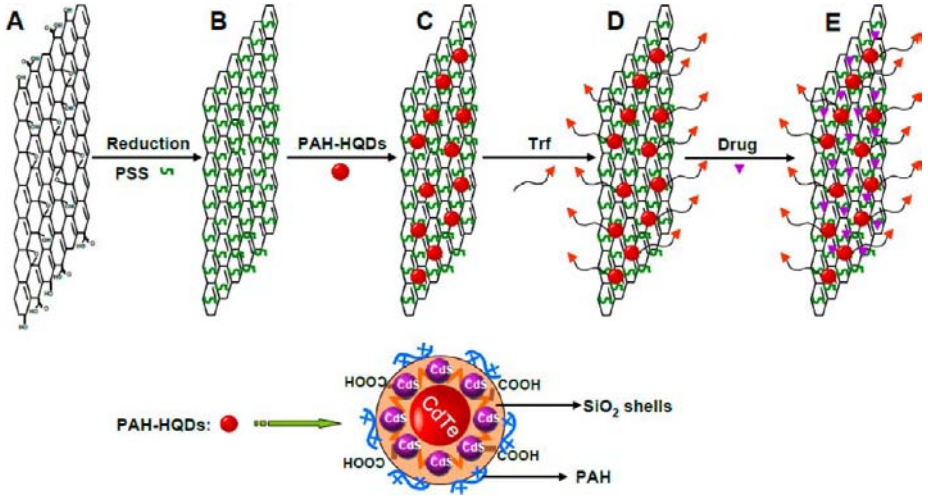

[a]A: GO. B: PSS coated graphene. C: graphene-HQDs. D: graphene-HQDs-Trf. E: DOX-graphene-HQDs-Trf.

Doxorubicin (DOX) is used as an example of anticancer drug, due to its fluorescence capability and its wide use in the treatment of a broad spectrum of tumors. The fluorescent graphene-HQDs carry DOX by $\pi-\pi$ stacking and hydrophobic interactions. After the fluorescent delivery nanosystem was taken by the cancer cells, the different fluorescence colors of graphene-HQDs and DOX excited by blue light are utilized to track and monitor the process of drug delivery and localize the graphene-HQDs. This new fluorescent delivery nanoassembly is successfully used for the first time in synchronous in vitro imaging, cell targeting, monitoring of drug delivery, and therapy.

EXPERIMENTAL SECTION

Materials. Natural graphite powder is obtained from Sinopharm Chemical Reagent Co., China. Poly(allylamine) (PAH, M_w 15 000), poly (sodium 4-styrenesulfonate) (PSS, M_w 70 000), dimethyl sulfoxide (DMSO), and transferrin (Trf, T3309) are received from Aldrich (Milwaukee, MI, USA). 1-(3-Dimethylaminopropyl)-3-ethylcarbodiimide hydrochloride (EDC) is obtained from Shanghai Aladdin Reagent Co., Ltd. *N*-Hydroxysuccinimide (NHS) is received from Acros Organics (Thermo Fisher Scientific, New Jersey, USA). 3-(4,5-Dimethylthiazol-2-yl)-2,5-diphenyltetrazolium bromide (MTT) assay kit is purchased from Nanjing KeyGEN Biotech Co., China. Doxorubicin hydrochloride (DOX) is purchased from Shanghai Sangon Biotech Co. DMEM (high glucose) cell culture medium, penicillin, trypsin, and streptomycin are purchased from Gibco Invitrogen. The other chemicals, e.g., sodium chloride, tetraethyl orthosilicate (TEOS), hydrazine hydrate, and thioglycolic acid (TGA) are obtained from National Medicines Corporation Ltd., China. Deionized (DI) water of 18 MΩ·cm is used throughout.

Characterizations. UV−vis spectra are recorded on a U-3900 spectrophotometer (Hitachi, Japan). Fluorescence spectra are measured on an F-7000 fluorescence spectrometer (Hitachi, Japan). Surface charge analysis and dynamic light scattering (DLS) are investigated by measuring zeta potential with a Nano Zetasizer (Malvern, England). XPS analysis is performed on an ESCALAB 250 surface analysis system (Thermo Electron). Raman spectra are measured on a HR-800 confocal microspectrometer (Horiba, Japan) with 633 nm laser excitation. TEM images are obtained with a field-emission transmission electron microscope at an accelerating voltage of 200 kV (JEM-2100F, JEOL, Ltd., Japan). Cell viability is assessed by MTT assay with multidetection microplate reader (μQuant, Biotek) at 570 nm. Cell image after taking up the graphene-HQDs is recorded on an inverted fluorescent microscope (Leica, blue and green excitation). The determination of tellurium (Te) in HQDs and graphene-HQDs is conducted by using an Agilent 7500a inductively coupled plasma mass spectrometer (ICP-MS, Agilent Technologies Inc.). HPLC analyses are performed with a Agilent 1200 HPLC system (Agilent Technologies Inc.) by using a C_{18} column 4.6 mm × 150 mm (5 μm) at a flow rate of 1 mL/min. Isocratic elution is employed using mobile phase of 50 mM potassium dihydrogen phosphate, in which acetonitrile (60:40) is injected for the recovery of DOX.

Graphene Oxide (GO) Preparation, Reduction, and Functionalization. GO is prepared by oxidizing graphite following the Hummers method.[17] It is then coated with PSS by reduction of 1 mg mL^{-1} exfoliated GO with hydrazine hydrate in 10 mg mL^{-1} PSS under reflux at 100 °C to produce reduced GO, i.e., PSS coated reductive GO (RGO). Afterward, the excessive PSS is removed by centrifugation/redispersion three times, and the obtained PSS coated RGO is dispersed in DI water by stirring and ultrasonication. The PSS amount coated on the surface of RGO is calculated by indirect determination of the content of sulfonate in GO-PSS by acid−base titration.[18] GO-PSS (9.625 mg) is first sonicated in HCl aqueous solution (500 μL, 0.1 mol L^{-1}) under argon protection for 40 min; the solution is then stirred for 48 h. The mixture is afterward placed into a dialysis chamber. Dialysis is continued until the dialysate becomes neutral. The dialysate is condensed using a rotary evaporator and titrated with 0.1 mol L^{-1} NaOH to reach the neutral point (pH 7.0), as monitored by a pH meter. A sulfonate content of 0.035 mmol was derived for the GO-PSS. 7.212 mg of PSS is derived in GO-PSS and a conjugation ratio of 3 is determined by calculating the weight of PSS and GO in the GO-PSS.

Preparation of HQD Nanoparticles. HQD nanoparticles are obtained by using a previously reported procedure. [13] The preparation of HQDs includes the following steps, i.e., 2.5 mL thioglycolic-capped CdTe nanocrystals (C_{Te} = 0.4 mmol L^{-1} derived from ICP-MS analysis) is precipitated by 2-propanol

dx.doi.org/10.1021/bc3004809 | *Bioconjugate Chem.* 2013, 24, 387−397

and redispersed in 50 mL aqueous solution of Cd^{2+} (1.65 mL, 0.1 M) and 36 μL TGA (pH 11.2, adjusted using 1 M NaOH). Diluted ammonia (0.5 mL, 6.25 wt%) and TEOS (0.49 mL) are mixed with the redispersed CdTe colloidal solution in a beaker which is sealed to minimize ammonia evaporation during incorporation. After being stirred for 3 h, the CdTe nanoparticle are coated with a thin SiO_2 layer containing Cd^{2+} and TGA. Then, a reflux process using this solution caused CdS-like clusters to nucleate and grow in the SiO_2 shells. Various refluxing times are adopted to obtain different-colored fluorescence of HQDs. The resultant product is finally filtered using a 0.22 μm filter to remove the composite fibers that are created simultaneously during the reflux.

PAH Capping HQDs (PAH-HQDs). The multicolour fluorescence of HQD nanoparticles (2 mL C_{Te} = 0.02 mmol L^{-1}) is precipitated by 2-propanol and sonicated in PAH solution (1 mL, 10 mg mL^{-1}) for 20 min. The multicolored fluorescence of PAH-HQDs are collected and purified with 2-propanol by ultracentrifugation to remove free PAH, then collected and redispersed in aqueous solution for future use. The PAH capping QD nanoparticles (PAH-QDs) were prepared in the same way as that described above for the PAH-HQDs by replacing QDs for HQDs.

PAH-HQDs Conjugation with Graphene. One milliliter of PAH-HQDs solution is added into 1 mL of PSS coated RGO aqueous solution (60 μg mL^{-1}) and 100 μL of NaCl (0.2 mol L^{-1}) and incubated at 37 °C for 2 h. The multicolored fluorescence of PAH-HQDs conjugated RGO (graphene-HQDs) is then obtained by centrifuging at 6000 rpm for 5 min followed by rinsing with ultrapure water three times, and the final graphene-HQDs are resuspended into ultrapure water for future use (graphene-HQDs-1, λ_{em} 560 nm; graphene-HQDs-2, λ_{em} 590 nm; and graphene-HQDs-3, λ_{em} 620 nm). ICP-MS analysis of tellurium (Te) at m/z 125 is adopted for the quantification of HQDs in the graphene-HQDs conjugate,[19] with blank controls and HQDs spiking recoveries. 13.5 μmol L^{-1} (C_{Te}) is derived in the graphene-HQD conjugate. The PAH-QDs conjugation with graphene (graphene-QDs) is prepared in the same way as that described above for the graphene-HQDs by replacing graphene-QDs for graphene-HQDs.

Preparation of the Graphene-HQDs-Trf Conjugates. Trf (10 μL, 10 mg mL^{-1}) reacts with EDC (10 μL, 10 mg mL^{-1}) at pH 5.5 in PBS buffer for 10 min, in the dark, at room temperature. Then, NHS (10 μL, 10 mg mL^{-1}) is added to EDC-Trf and reacted for 20 min. The formed amine-reactive Trf-NHS ester further reacted with graphene-HQDs at pH 7.4 in PBS for 3 h in the dark to get a stable amide bond resulting in the formation of the graphene-HQDs-Trf. The excessive reagents are then removed by discarding the supernatant after centrifugation and the graphene-HQDs-Trf is washed for 3 times with DI water and finally redispersed in fresh PBS and stored at 4 °C for future use. To evaluate the Trf conjugation ratio, the supernatant and the washed solutions were collected and the residual Trf content is obtained by measuring the complex formed between Trf and Coomassie brilliant blue at 575 nm by UV−vis spectrophotometry.[20] A conjugation ratio of 0.1 is achieved by calculating the weight of conjugated Trf and graphene-HQDs in the graphene-HQDs-Trf.

DOX Loading onto the Graphene Nanoassembly. DOX hydrochloride (1 mM) is stirred with graphene-HQDs-Trf, graphene-HQDs in PBS buffer at various pH values for 24 h in the dark at room temperature. The products denoted as DOX-graphene-HQDs-Trf, DOX-graphene-HQDs are collected by repeated ultracentrifugation with PBS until the supernatant become free of reddish color (corresponding to DOX-free), and then resuspended and stored at 4 °C. To evaluate the DOX-loading factor (LF, defined as the mass ratio of DOX to graphene nanoassembly), the supernatant, and the washed solutions were collected, and the residual DOX (W_{rDOX}) content is obtained by measuring the absorbance at 490 nm (the characteristic absorbance of DOX) relative to a calibration curve recorded under the same conditions as shown in Figure S1. The loading factor (LF) of DOX is expressed as $LF = (W_{DOX} - W_{rDOX})/W_{graphene\text{-}HQDs\text{-}Trf}$, where W_{DOX} is the original DOX amount, while $W_{graphene\text{-}HQDs\text{-}Trf}$ is the weight of the graphene-HQDs-Trf.

Drug Release Behaviors of DOX-Graphene-HQDs-Trf Conjugates. The DOX-graphene-HQDs-Trf is dispersed into PBS buffer (2 mL) at various pH values at 37 °C in the dark. After different time intervals, the graphene nanoassemblies are separated from the buffer by ultracentrifugation, and the concentration of the released DOX in the supernatant is estimated by UV−vis spectroscopy. The concentrations of the released drug are calculated by the Beere-Lambert Law according to the absorbance of the release media at a certain characteristic adsorption wavelength.

Cell Culture. HeLa cells and HEK293 human kidney cells are maintained in a DMEM medium containing 10% fetal bovine serum, 100 U mL^{-1} penicillin, and 100 μg mL^{-1} streptomycin. Cell culture is cultivated in a complete medium at 37 °C in a humidified environment of 5% CO_2. The cells are harvested from subconfluent cultures by using trypsin/EDTA solution (5%) and are resuspended in fresh complete medium before plating.

Cell Viability Assay. The effect of graphene-HQD suspensions on in vitro viability of cells is assessed by MTT reduction assay. Cells are plated in 100 μL DMEM at a density of 1000 cells in a 96-well plate. After incubation overnight to allow the cells to attach on the plate, a 10 μL portion of the DOX-graphene-HQDs-Trf, graphene-HQDs-Trf, DOX-graphene-HQDs, and DOX with various concentrations is added to each well, and incubation is carried out for 24, 48, and 72 h in 5% CO_2 at 37 °C. Afterward, 50 μL of MTT (1 mg mL^{-1} in PBS) is added to the culture in each well followed by incubation for 4 h. The medium is then replaced with 150 μL dimethyl sulfoxide, and the absorbance is monitored with a microplate reader at 570 nm. A linear relationship between cell number and optical density is established, and the cell viability ratio is calculated according to A570 nm/A570 nm(control).

In Vitro Cellular Studies. For cells incubated with the DOX-loaded graphene nanoassembly, HeLa cells are cultured 24 h to allow attachment, washed with pH 7.4 PBS, and then incubated with DOX-graphene-HQDs-Trf, graphene-HQDs-Trf, and graphene-HQDs at 37 °C for 1, 4, 12, and 24 h separately in DMEM medium. After incubation, the cells are washed repeatedly with sterilized PBS before further analysis. To further evaluate the role of Trf in the cellular uptake of graphene-HQDs-Trf, the HEK293 cells are cultured with graphene-HQDs-Trf for 4 h washed with sterilized PBS and analyzed by an inverted fluorescence microscopy. For the purpose of imaging, the cells are pretreated with free Trf (2 μM) for 2 h followed by adding graphene-HQDs-Trf and further culturing for 4 h. Fluorescence imaging is performed after washing with sterilized PBS (blue excitation for graphene-HQDs imaging and green excitation for DOX imaging).

dx.doi.org/10.1021/bc3004809 | Bioconjugate Chem. 2013, 24, 387−397

RESULTS AND DISCUSSION

Preparation and Stability of the DOX-Graphene-HQDs-Trf. The synthetic strategy of DOX-graphene-HQDs-Trf is shown in Scheme 1. Electrostatic attraction is the main driving force for the conjunction of positively charged PAH-capped HQDs nanoparticles with NH_2 (or NH_3^+) groups and negatively charged PSS-capped graphene with $-SO_3H$ ($-SO_3^-$) groups. In the present work, Trf conjugated graphene-HQDs are used to target the HeLa cells. Trf is "activated" into an amine reactive succinimide ester using carbodiimide cross-linker moleculer of EDC and NHS, followed by reacting with the amine groups on the surface of graphene-HQDs. Subsequent mixing of the graphene-HQDs-Trf with DOX in PBS buffer allows the DOX to be attached to the graphene sheets.

The zeta potential of the graphene nanoassembly changes dramatically following the synthetic strategy (Table 1). At first, graphene-PSS has a negative potential due to the presence of $-SO_3^-$ groups of PSS on the sheets, and the potentials converted to positive after deposition of PAH-HQDs, indicating adsorption of PAH-HQDs onto the graphene-PSS. Although Trf is an acidic protein carrying a net negative charge at a pH exceeding its p*I* value (pI_{Trf} = 5.9),[21] graphene-HQDs-Trf in aqueous solution (at pH 7) shows a zeta potential of +(8.3 ± 0.5) mV. The positive value is probably due to the presence of free amine groups of PAH without coupling to Trf. After adsorption of cationic DOX, the zeta potential is slightly increased to +(8.8 ± 0.4) mV, showing no obvious change compared with that of graphene-HQDs-Trf. This indicated that little DOX is absorbed on the surface of graphene-HQDs-Trf, while most DOX is adsorbed on the surface of graphene by $\pi-\pi$ stacking and hydrophobic interaction. In the present case, $\pi-\pi$ stacking interaction and hydrophobic interaction play important roles with respect to the DOX loading.

Table 1. Zeta Potential Values for the Graphene Nano-Assembly

material	zeta potential (mV)
Graphene-PSS	−37.6 ± 1.2
PAH-HQDs	+42.3 ± 2.1
Graphene-PSS-PAH-HQDs	+31.0 ± 3.7
Graphene-PSS-PAH-HQDs-Trf	+8.3 ± 0.5
DOX-graphene-PSS-PAH-HQDs-Trf	+8.8 ± 0.4

GO reduction and formation of polymer-coated graphene are confirmed by Raman and UV−vis spectra. In Figure S2a, peak D is due to first-order zone boundary phonons observed for defected graphene, while peak G is caused by in-plane optical vibration (degenerate zone center E2g mode). [22] The D/G intensity ratio is an indication of disorder in graphene.[23,4] A ratio of 1.36 for graphene-PSS with respect to 1.07 for GO is attributed to a local disorder band induced by chemical reduction.

Figure S2b shows strong absorptions of GO centered at 230 and 300 nm, corresponding to $\pi-\pi^*$ transitions of aromatic C═C and $n-\pi^*$ transitions of C═O in GO, respectively. A red-shift from 230 to 268 nm of the absorption of graphene-PSS indicates restoration of the electronic conjugation within graphene sheets after reduction. With respect to the absorption of fully reduced graphene sheets at 270 nm, [24] it is conclusive that graphene-PSS is almost completely reduced. On the other hand, the absorption of PSS at 223 nm is shifted to 226 nm in graphene-PSS due to the interaction between GO and PSS, indicating strong attachment of PSS onto the surface of graphene.

Figure 1A illustrates UV−vis spectra of Trf, graphene-HQDs, graphene-HQDs-Trf, and DOX-graphene-HQDs-Trf. The absorption at 280 nm from Trf is clearly observable for graphene-HQDs-Trf and DOX-graphene-HQDs-Trf, proving successful conjugation of Trf on graphene-HQDs. DOX displays absorptions at 490 and 232 nm,[25] and these two absorptions are slightly red-shifted after DOX adsorption on graphene-HQDs-Trf, indicating interactions between DOX and graphene-HQDs-Trf. The reddish color of the DOX-graphene-HQDs-Trf offers further evidence for the formation of bound DOX-graphene complexes as reflected by its characteristic absorption at 503 nm (Figure 1A-b).

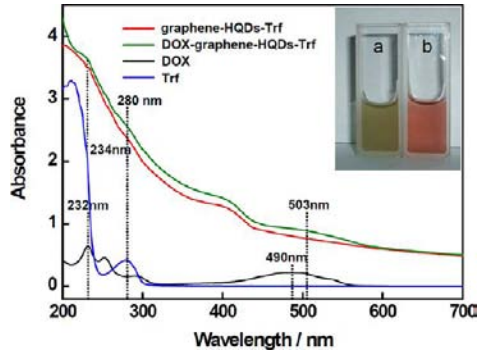

Figure 1. UV−vis absorption spectra. Inset: photograph of graphene-HQDs-Trf solutions without (a) and with (b) bound DOX.

XPS analysis provided further information for GO conversion to graphene-PSS (Figure 2), according to the diminished C (epoxy/ether), C—OH, C═O content, and the increased C—C, C—S signal from PSS. Figure S3 illustrated that the component peaks at 405.4, 412.1 eV and 572.8, 583.3 eV correspond to Cd3d and Te3d, respectively, while the peak at 103 eV is due to SiO_2 from HQDs and that at 399.9 eV is attributed to N1s from PAH. These peaks are entirely absent for graphene-PSS and all come from PAH-HQDs, proving the successful conjugation of graphene-PSS and PAH-HQDs.

Figure 3 illustrated the TEM images of the HQD assemblies. The HQDs uniformly distributed on graphene-PSS (Figure 3b), evidencing the well-behaved assembly process. The energy-dispersive X-ray spectrum (EDX) in Figure 3c confirmed the existence of the elements C in graphene, and Cd, Te, Si, O, and N in the hybrid SiO_2−CdTe, and the element Cu comes from the lacey support film. There are no obvious element peaks due to the single sheet of graphene and the low content of HQDs. The element signals from the graphene and HQDs are consistent with the TEM observations.

The stability of the graphene-HQDs is investigated using PL intensity and DLS. The optical images in Figure 4a,b show that the graphene-HQDs emit very strong PL under UV irradiation, and have a good aqueous dispersibility with no aggregation. In addition, no significant change in particle size of the graphene-HQDs in aqueous solution was observed (Figure 4c). Further, the dispersion of graphene-HQDs is stable over a wide range of salt concentration and pH values. As shown in Figure 4d, the increase in salt concentration up to 300 mM resulted in no obvious variation of the fluorescence intensity in 6 days. Even the fluorescence intensity gradually decreased to ca. 60% of the

dx.doi.org/10.1021/bc3004809 | Bioconjugate Chem. 2013, 24, 387−397

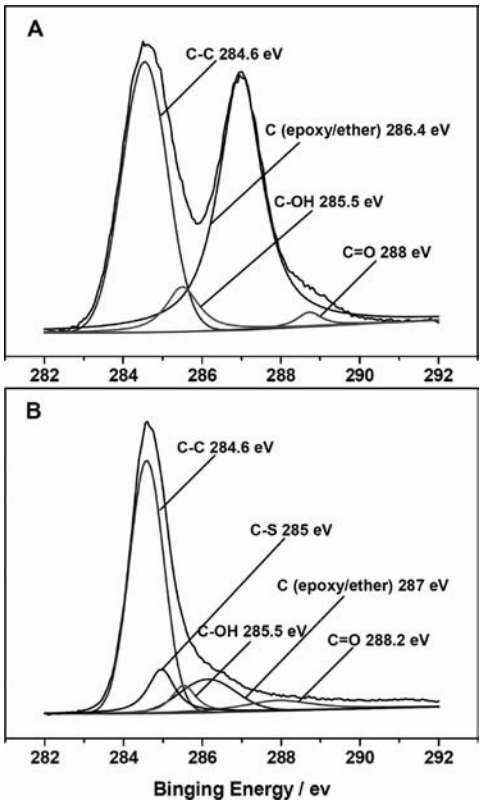

Figure 2. High-resolution XPS curves of carbon in (A) GO and (B) graphene-PSS.

original level in the presence of >300 mM salt after 6 days, the graphene-HQDs can still be used as fluorescent nanoprobe for intracellular imaging as the salt concentration in the human body is far below 300 mM. The dependence of relative PL intensity on pH as illustrated in Figure 4e showed that the PL intensity remains virtually constant in the pH range 3−10 within a long time of 6 days. This indicates that graphene-HQDs are insensitive to the variation of pH, and this is of particular interest for its applications as intracellular imaging probes and drug carriers, because most intracellular organelles such as endosomes are acidic at pH 4−6. The excellent stability of graphene-HQDs might be attributed to HQDs; hybrid SiO_2 shells make QDs less sensitive to the surrounding chemicals and more biocompatible.[13]

The stability of graphene-HQDs is further investigated in water, NaCl, PBS, bovine serum albumin (BSA), and DMEM (high glucose, 10% serum-containing) media for 4 h incubation at 37 °C. Figure 4f shows that graphene-HQDs exhibited excellent stability in these biological solutions. Figure 4g shows that graphene-HQDs exhibited strong light emission under UV radiation in these media under investigation, proving that these media pose no suppressions on the emission of graphene-HQDs. Thus, the graphene-HQDs possess favorable aqueous dispersion properties and excellent stability, which are the prerequisites when acting as drug carrier and probe for intracellular imaging and monitoring the process of drug delivery.

Luminescent Properties of Graphene-HQDs. Figure 5a shows the fluorescent emission spectrum of multicolored graphene-HQDs with narrow emission band (graphene-HQDs-1, λ_{em} 560 nm; graphene-HQDs-2, λ_{em} 590 nm; and graphene-HQDs-3, λ_{em} 620 nm). As shown in Figure S4, the prepared graphene-HQDs still possess strong fluorescence even after the HQDs conjugated with graphene, a strong fluorescence quencher. As a comparison, the fluorescence of CdTe QDs and graphene-QDs are also shown in Figure S4. The fluorescence of QDs is almost completely quenched when attaching on the surface of graphene; this means the polymers (PSS and PAH) coated on the surface of graphene and HQDs could not protect the fluorescence from being quenched by graphene. The results herein indicated that the SiO_2 shells coated on QDs play an important role in maintaining the fluorescence property of HQDs, and endow graphene with attractive luminescent properties with a PL quantum yield of 12%.

The PL decay curve of HQDs is well-described by two exponential functions with an average lifetime of 23.3 ns (Figure 5b). After conjugating with graphene, graphene-HQDs exhibit an average lifetime of 8.0 ns. It has been reported in the literature that the average lifetime of CdSe/ZnS QDs on Au substrate is less than 1 ns[26] and PEI-capped CdSe/ZnS QDs on magnetite nanorings for multiphoton fluorescence and magnetic resonance imaging is 7 ns. [27] In the present case, the slightly longer lifetime of the graphene-HQDs might be due to the recombination within closely packed HQDs and resonant energy transfer between the HQDs and graphene sheets. In this juncture, we have performed a control experiment for comparison, which give rise to average lifetimes of 16.0 ns and 224.5 ps for CdTe QDs and graphene-QDs, respectively (the decay curves of which are shown in the Supporting Information, Figure S5). These results indicated that the prepared graphene-based nanoassembly endows graphene with excellent fluorescent property, and the graphene-HQDs could serve as an effective probe for intracellular imaging and tracking delivery of the drug.

DOX Loading on the Graphene Nanoassembly and Its Subsequent Release. The fluorescent graphene nanoassembly is loaded with drug by mixing with DOX in PBS buffer overnight and the excessive or unbound DOX is removed by filtration. It is interesting to see that the amount of DOX bound onto graphene is pH-dependent (Figure 6a). A loading factor of 0.5 is achieved at pH 5.5, while it is increased to 1.0 and 1.4 when enhancing to pH 7.4 and pH 8.5, respectively. The improvement on the adsorption of DOX at higher pH is due to its increased hydrophobicity caused by decreased protonation of cationic groups ($-NH_2$) in it. This enhances hydrophobic interaction between DOX and the graphene nanoassembly.[25] The original DOX and that recovered by elution from the DOX-graphene-HQDs-Trf are analyzed by HPLC with spectrophotometric detection at 490 nm to investigate whether it is degraded during the loading and releasing process. The HPLC chromatograms are shown in Figure S6. No degradation is observed, although a slight difference for the retention time is recorded for the original DOX and that recovered by elution, i.e., a retention time of 1.752 min (Figure S6A) is assigned for DOX while that for the recovered DOX is 1.873 min (Figure S6B). This observation is consistent with the results demonstrated in a previous report.[28]

The loading capacity of DOX on graphene-HQDs-Trf is estimated to be 1.4 mg mg^{-1} as illustrated in Table S1. This value is lower than that of the folic acid-nano GO with bare graphene as drug vehicle,[29] while it is much higher than those of other common drug vehicles, including Fe_3O_4 modified graphene oxide (1.08 mg mg^{-1}),[16] micellar hybrid nanoparticle,

dx.doi.org/10.1021/bc3004809 | Bioconjugate Chem. 2013, 24, 387−397

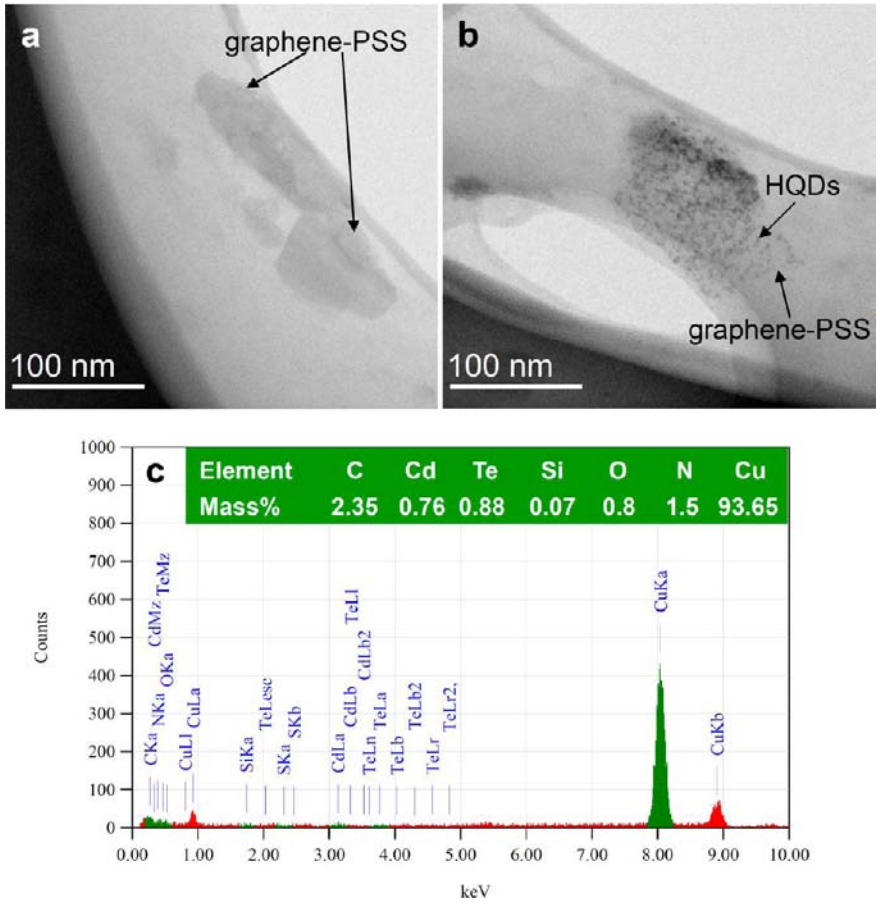

Figure 3. TEM images of (a) graphene-PSS and (b) graphene-HQDs. (c) EDX spectrum acquired from graphene-HQDs.

and mesoporous silica nanoparticles, where the loading capabilities are well below 1 mg mg^{-1}.[30−32]

Figure 6b illustrates the release of drug from DOX-loaded graphene-HQDs-Trf nanocomposite measured in PBS buffer at 37 °C at pH 5.5, 7.4, and 8.5. It is evident that the release of DOX is highly pH dependent. The DOX on the graphene nanoassembly support is stable in PBS buffer at pH 7.4 and 8.5 at 37 °C, while a larger amount of DOX is released at pH 5.5, corresponding to the endosome pH. This is attributed to the increased hydrophilicity and solubility of the protonated DOX at this pH.[33] On the other hand, only ca. 65% of the loaded DOX is released from the carriers at pH 5.5. This is an obvious indication of sustainable drug release of the DOX-graphene-HQDs-Trf system. The kinetics of the system are exactly what we expected for the cases when a high initial dose is required followed by slow release of the drug with smaller dose.

Fluorescence Imaging and Cell Uptake of Graphene-HQDs-Trf. HeLa cells are directly labeled through specific recognition between the Transferrin receptors on cell membrane and the Trf ligand conjugated with the graphene-HQDs surface. Trf negative HEK293 cells incubation with graphene-HQDs-Trf negative control experiment is used for comparison. Figure 7a shows fluorescent microscopic images of HEK293 cells treated with graphene-HQDs-Trf-3 for 4 h incubation, followed by copious wash steps to remove unbound graphene-HQDs-Trf-3 before fixing on coverslips for imaging. The red-emitting nanoparticles are found randomly distributed with no specific interaction or attachment with the cell membrane even after 4 h of incubation. This suggests a minimal nonspecific interaction of graphene-HQDs-Trf-3 with the cell membrane. As another control experiment, graphene-HQDs without conjugating Trf are incubated with HeLa cells, and slight red emission is observed (Figure 7b). To evaluate the role of Trf in the cellular uptake of graphene-HQDs, the Trf receptor was blocked by pretreating the Hela cells with free Trf for 2 h. As shown in the Figure 7c, a much weaker red emission is observed, demonstrating a competitive uptake of graphene-HQDs-Trf and Trf by the cells. This suggests that the graphene-HQDs-Trf is internalized via the Trf receptor-mediated pathway. However, a dramatic change is observed when graphene-HQDs-Trf is incubated with HeLa cells. The red-emitting graphene-HQDs-Trf-3 (Figure 7d,e) and green-emitting graphene-HQDs-Trf-1 (Figure S7) are able to make targeted label of the HeLa cells. It indicated that a high concentration of nanoparticles specifically attached to the HeLa cell membrane at 1 h incubation (Figure 7d). After 4 h incubation, most of the nanoparticles on the cell membrane disappear, while the red color is still observable (Figure 7e). This is attributed to the fact that the graphene-HQDs-Trf attached on the cell membrane are taken up by the HeLa cells and transferred into the endosomes, while the cells maintain their characteristic polygonal morphology and well-spread pattern. Similarly, the green-emitted nanoparticles almost completely decorated the cell membrane with 1 h incubation (Figure S6a). After investigating the images of 24 h incubation (Figure S7b), it is conclusive that the cell proliferation is not hindered when HeLa cells are exposed to the graphene-HQDs-Trf for a long time. These observations further indicate that the

dx.doi.org/10.1021/bc3004809 | Bioconjugate Chem. 2013, 24, 387−397

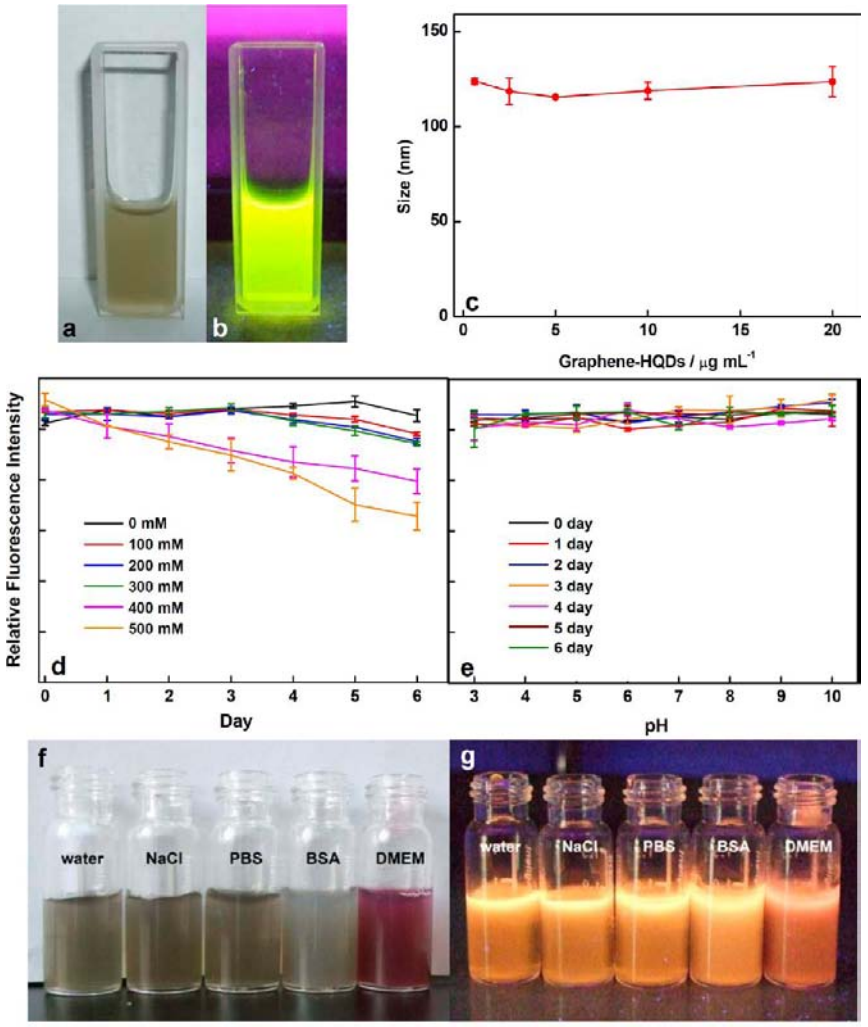

Figure 4. Optical images of graphene-HQDs-1 in aqueous solution (a, in ambient condition; b, under UV irradiation); (c) the dependence of particle size of graphene-HQDs-1 on concentration; (d,e) the dependence of fluorescence intensity of graphene-HQDs on salt concentration and pH value; (f,g) digital photographs for the dispersion status of graphene-HQDs-2 in water, NaCl (300 mM), PBS (10 mM, pH 7.4), BSA (10 g L^{-1}), and DMEM (high glucose, 10% serum) for 4 h incubation at 37 °C (f, in ambient condition; g, under UV irradiation).

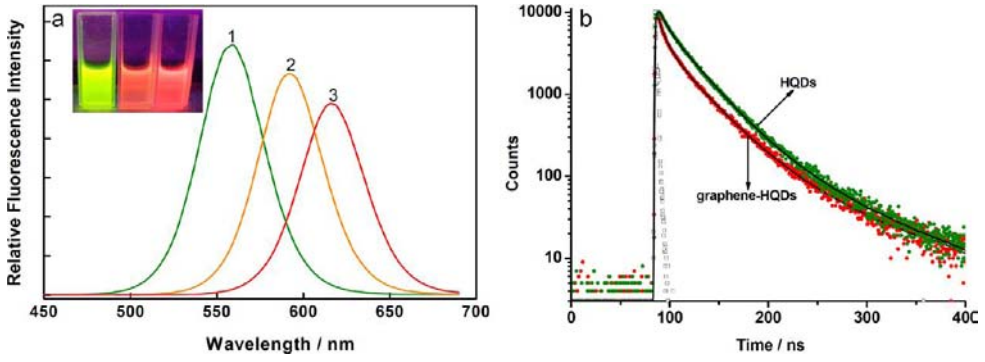

Figure 5. (a) Fluorescence spectra of (1) graphene-HQDs-1, (2) graphene-HQDs-2, (3) graphene-HQDs-3 (Inset: photographs of graphene-HQDs solutions under UV irradiation). (b) PL decay curves of HQDs and graphene-HQDs-3.

incubation of HeLa cells with the fluorescent graphene-HQDs-Trf causes virtually no harmful effect to the essential activities of HeLa cells, e.g., cell attachment, spread, mitosis, and proliferation. [34] In other words, the nanoassembly of graphene-HQDs-Trf is an ideal prerequisite material acting as diagnostic contrast agents. Furthermore, conjugating near-infrared emitting HODs on the surface of graphene might facilitate much brighter imaging for in vivo applications.

To future evaluate whether the graphene-HQDs-Trf are internalized in the HeLa cells, rather than being simply bound to the cell surface, TEM images were taken for this purpose. After incubating with graphene-HQDs-Trf, aggregation of graphene is observed as black patches inside the cell cytoplasm

dx.doi.org/10.1021/bc3004809 | *Bioconjugate Chem.* 2013, 24, 387−397

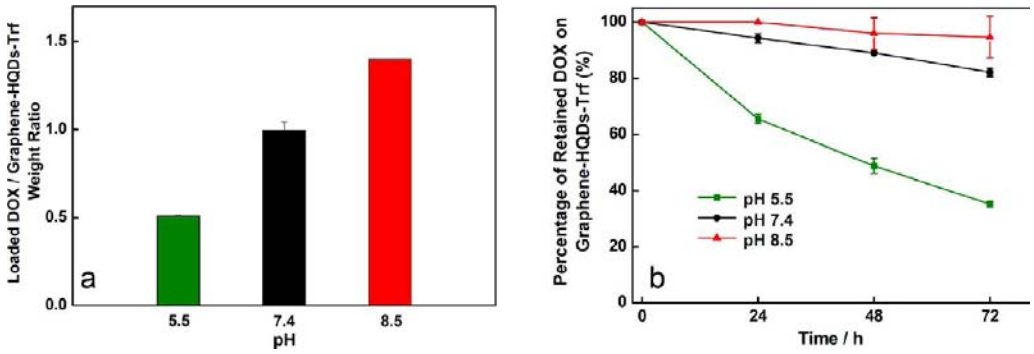

Figure 6. pH-dependent loading and release of DOX on the graphene nanoassembly: (a) drug loading efficiency of the graphene nanoassembly; (b) DOX release in PBS buffer at 37 °C.

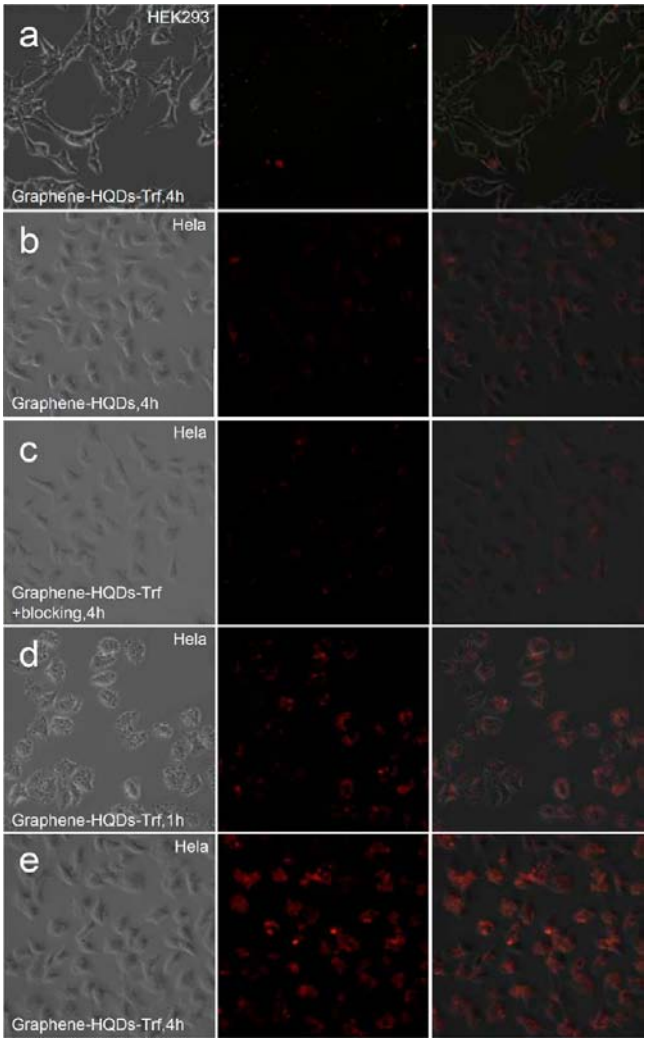

Figure 7. Fluorescent microscopic images of HEK293 cells directly labeled by graphene-HQDs-Trf-3 for 4 h (a); HeLa cells incubated with (b) graphene-HQDs-3 for 4 h, (c) Trf for 2 h followed by graphene-HQDs-Trf-3 for 4 h, graphene-HQDs-Trf-3 for 1 h (d) and 4 h (e). Left: the bright-field images. Middle: the fluorescent images. Right: the merged images of the left and middle ones.

(Figure 8b,c). The graphene particles are first localized in vesicles after endocytosis (Figure 8b), and then they disrupt the phospholipid membrane, escape from endosomes, and release into the cytoplasm (Figure 8c). On observing the cell morphology, it seems that the majority of the internalized

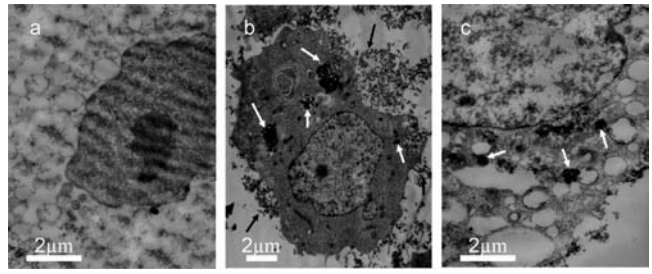

Figure 8. TEM images of (a) bare HeLa cells and (b,c) graphene-HQDs-Trf-3 treated HeLa cells. In (b), graphene-HQDs-Trf-3 is stored in endosomes, while in (c) it escapes from endosomes and releases into the cytoplasm. The white arrows point to the aggregated graphene-HQDs-Trf-3 inside Hela cells, and the black arrows point to graphene-HQDs-Trf-3 outside HeLa cells.

graphene accumulates inside the endosomes. This indicates that graphene-HQDs-Trf could be a favorable intercellular imaging probe with the ability of cell penetration.

Cellular Uptake of the DOX-graphene-HQDs-Trf. The DOX loaded graphene-HQDs-Trf-1 is incubated with HeLa cells for different periods of time at 37 °C, followed by copious wash steps to remove the unbound DOX-graphene-HQDs-Trf-1. After incubation of the HeLa cells, the graphene-HQDs-Trf-1 and the released DOX are localized by analyzing with fluorescence microscopy, as the graphene-HQDs-Trf-1 and the DOX emit green and red fluorescence, respectively, under irradiation with blue and green light. In addition, DOX also emits orange fluorescence under blue light excitation. In combination with the green fluorescence of graphene-HQDs-Trf-1, it is feasible to record the dual-colored fluorescent images, leading to simultaneous observation of the graphene-HQDs-Trf-1 and DOX localization which facilitate inspecting the drug delivery and release process.

Figure 9b reveals that DOX-graphene-HQDs-Trf-1 is effectively taken up by HeLa cells. In comparison with the green fluorescence from HeLa cells incubated with graphene-HQDs-Trf-1 (Figure 9a-i), the stained HeLa cells emit slight yellow fluorescence. The overlap of the green fluorescence from graphene-HQDs-Trf-1 and the orange fluorescence from DOX illustrated that the graphene nanoassemblies mainly accumulate in the cytoplasm even with a longer incubation time of 6 h (Figure 9a-i). It is also apparent that the brighter red fluorescence from DOX, associated with graphene-HQDs-Trf-1, is mostly focused on the cytoplasm but not on the cell nuclei (Figure 9ii), whereas free DOX can diffuse and penetrate into the cell and nuclei membrane, quickly accumulate inside the

dx.doi.org/10.1021/bc3004809 | Bioconjugate Chem. 2013, 24, 387−397

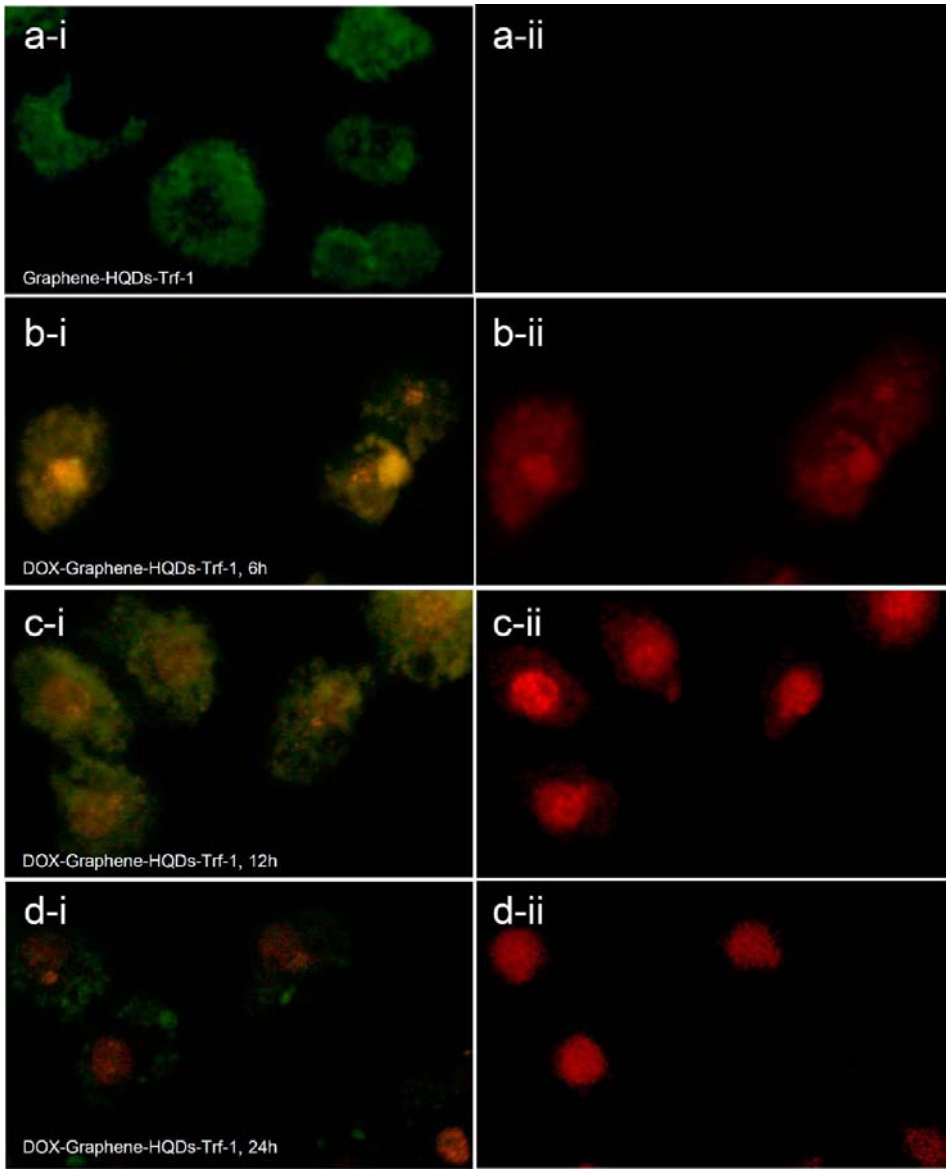

Figure 9. Fluorescent microscopic images of HeLa cells directly labeled by graphene-HQDs-Trf-1 for 4 h (a), and DOX-graphene-HQDs-Trf-1 for 6 h (b), 12 h (c), and 24 h (d). (i, fluorescent images by blue light excitation; ii, fluorescent images by green light excitation.)

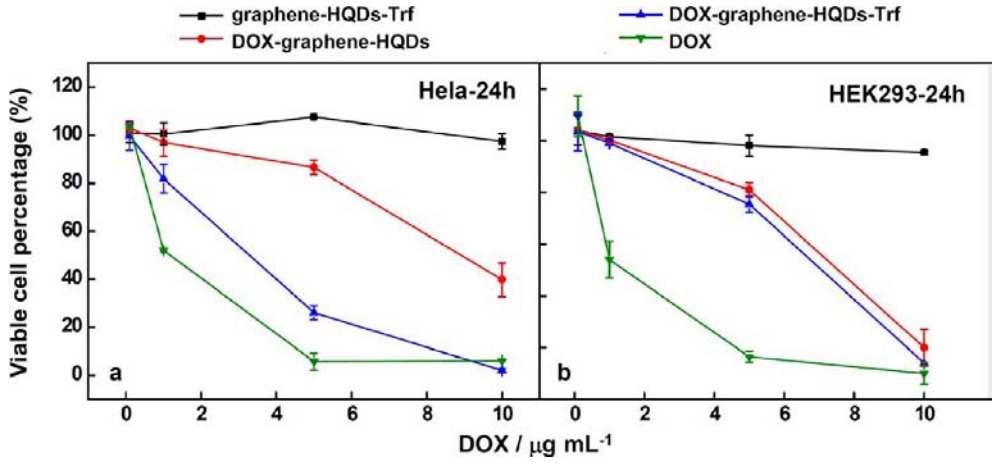

Figure 10. Concentration dependent survival curves of HeLa cells (a) and HEK293 cells (b) treated by various graphene nanoassemblies for 24 h. Cells were seeded on 96-well culture plates at an initial density of 1000 cells/well; the viable cell percentage was measured by MTT assay.

dx.doi.org/10.1021/bc3004809 | *Bioconjugate Chem.* 2013, 24, 387−397

nuclei, and intercalate into the DNA helix.[35] The above observations demonstrate the efficient internalization of the graphene-HQDs-Trf-1, which carry DOX into the cells most likely through the receptor-mediated endocytosis mechanism.

After 12 h incubation of HeLa cells with DOX-graphene-HQDs-Trf-1 (Figure 9c), the loaded DOX produced fluorescence in both the nuclei and cytoplasm, demonstrating that DOX might be released to the cytoplasm and eventually enter the cell nuclei. After 24 h internalization, the loaded DOX is mostly found in the cell nuclei (Figure 9d-ii), where DOX is known to interact with topoisomerase II to cause DNA cleavage and cytotoxicity.[35] Meanwhile, graphene-HQDs-Trf-1 is still found only in the cytoplasm, indicating that it cannot penetrate into the cell nuclei membrane (Figure 9d-i). The cytoplasm of the stained HeLa cells shows a fluorescence color change from slight yellow to green, and the orange fluorescence from the cell nuclei becomes brighter, while the red emission of DOX gradually focuses on the cell nuclei from the cytoplasm when extending the incubation time (Figure 9b-ii, c-ii, d-ii). This indicates that DOX release from DOX-graphene-HQDs-Trf-1 is sustainable in accordance with the results of our drug releasing experiment above.

Cytotoxicity Test. After having confirmed the feasibility of using DOX-graphene-HQDs-Trf for cancer cell imaging, we further examined its in vitro cellular cytotoxicity to HeLa and HEK293 cell lines as compared to graphene-HQDs, DOX-graphene-HQDs, and DOX alone. The MTT assay results demonstrate that graphene-HQDs-Trf with different concentrations caused negligible cytotoxicity on HeLa cell viability after incubation for 24 h (Figure 10a).

It is also seen that DOX-graphene-HQDs and DOX-graphene-HQDs-Trf have lower toxicity effect than free DOX on both types of cells. The latter exhibits increased toxicity to HeLa cells than to that of HEK293 cells, owing to specific Trf receptor recognition and thus enhanced cellular uptake of the graphene drug. Figure 10b indicated that the graphene-HQDs show insignificant toxicity for HEK293 cells at various concentrations, and DOX-graphene-HQDs and DOX-graphene-HQDs-Trf show similar effect on HEK293 cell viability. The conjugation of Trf onto DOX-graphene-HQDs gives no obvious enhancement in intracellular DOX delivery. The concentration-dependent toxicity shows that both DOX-graphene-HQDs and DOX-graphene-HQDs-Trf have lower toxicity to HEK293 cells than free DOX. These observations suggest that Trf conjugation to graphene results in no variation on DOX delivery and causes no destruction for normal cell HEK293. The results indicated that this functionalized graphene nanosystem improves the safety of chemotherapy and exhibits obvious potential for selective increase of drug cytotoxicity to certain types of cells, e.g., Hela cells, by conjugation of targeting molecules as drug vehicles.

CONCLUSION

Graphene-HQDs as a new fluorescent nanocomposite facilitate simultaneous imaging/mapping of cancer cells, rendering targeted drug delivery, monitoring the process of drug release, and localizing the drug vehicle. This novel hybrid nanomaterial combines the advantages of graphene and HQDs and displays excellent stability and exhibit attractive fluorescence as well as extremely high drug loading efficiency. Thus, only low graphene-HQD concentrations are required for effective diagnostic and therapeutic applications, and in vitro toxicity data suggest minimal cytotoxicity for graphene-HQDs. Furthermore, the fluorescence color of graphene-HQDs can be changed by simply adjusting the size of HQDs. Both of the dual-colored fluorescent images and TEM results of cell samples improve the DOX-graphene-HQDs-Trf internalized by endosomes and followed by slow endosomal escape and release into the cytoplasm; DOX is efficiently released and enters the cell nucleus and induces HeLa cell death. Based on the control experiment, it is possible to conclude that the whole nanoscale drug system is selective and effective. Thus, graphene-HQDs could be used for biomedical applications including highly target-specific diagnosis, monitoring, and therapy. Furthermore, through the other conjugated disease-specific ligands, other targeting molecules, and other fluorescent therapeutic agents, similar multifunctional nanosystems may potentially be developed for additional important medical applications.

ASSOCIATED CONTENT

Supporting Information

Additional experimental data, spectra, and images. This material is available free of charge via the Internet at http://pubs.acs.org.

AUTHOR INFORMATION

Corresponding Author

*E-mail address: jianhuajrz@mail.neu.edu.cn (J.-H. Wang). Tel: +86 24 83688944. Fax: +86 24 83676698.

Notes

The authors declare no competing financial interest.

ACKNOWLEDGMENTS

The authors gratefully acknowledge financial support from the Natural Science Foundation of China (21275027, 21235001, and 21075013), the Program of New Century Excellent Talents in University (NCET-11-0071), the SRFDP program (20120042110020), and the Fundamental Research Funds for the Central Universities (N110705002, N110405005, and N110805001).

REFERENCES

(1) Liu, Z., Robinson, J. T., Sun, X., and Dai, H. (2008) PEGylated nanographene oxide for delivery of water-insoluble cancer drugs. *J. Am. Chem. Soc. 130*, 10876−10887.

(2) Zhang, Y., Nayak, T. R., Hong, H., and Cai, W. (2012) Graphene: a versatile nanoplatform for biomedical applications. *Nanoscale 4*, 3833−3842.

(3) Robinson, J. T., Tabakman, S. M., Liang, Y., Wang, H., Casalongue, H. S., Vinh, D., and Dai, H. (2011) Ultrasmall reduced graphene oxide with high near-infrared absorbance for photothermal therapy. *J. Am. Chem. Soc. 133*, 6825−6831.

(4) Wang, Y., Li, Z., Wang, J., Li, J., and Lin, Y. (2011) Biofunctionalization and applications in biotechnology. *Trends Biotechnol. 29*, 205−212.

(5) Yang, X., Zhang, X., Liu, Z., Ma, Y., Huang, Y., and Chen, Y. (2008) Superparamagnetic graphene oxide-Fe_3O_4 nanoparticles hybrid for controlled targeted drug carriers. *J. Phys. Chem. C 112*, 17554−17558.

(6) Eda, G., Lin, Y. Y., Mattevi, C., Yamaguchi, H., Chen, H. A., Chen, I. S., Chen, C. W., and Chhowalla, M. (2010) Blue photoluminescence from chemically derived graphene oxide. *Adv. Mater. 22*, 505−509.

(7) Essig, S., Marquardt, C. W., Vijayaraghavan, A., Ganzhorn, M., Dehm, S., Hennrich, F., Ou, F., Green, A. A., Sciascia, C., Bonaccorso, F., Bohnen, K. P., Lohneysen, H., Kappes, M. M., Ajayan, P. M., Hersam, M. C., Ferrari, A. C., and Krupke, R. (2010) Phonon-assisted

electroluminescence from metallic carbon nanotubes and graphene. *Nano Lett. 10*, 1589−1594.
(8) He, S., Song, B., Li, D., Zhu, C., Qi, W., Wen, Y., Wang, L., Song, S., Fang, H., and Fan, C. (2009) A graphene nanoprobe for rapid, sensitive, and multicolor fluorescent DNA analysis. *Adv. Funct. Mater. 20*, 453−459.
(9) Medintai, I. L., Uyeda, H. T., Goldmani, E. R., and Mattoussi, H. (2005) Quantum dot bioconjugates for imaging, labelling and sensing. *Nat. Mater. 4*, 435−446.
(10) Shi, D., Guo, Y., Dong, Z., Lian, J., Wang, W., Liu, G., Wang, L., and Ewing, R. C. (2007) Quantum-dot-activated luminescent carbon nanotubes via a nano scale surface functionalization for in vivo imaging. *Adv. Mater. 19*, 4033−4037.
(11) Dong, H., Gao, W., Yan, F., Ji, H., and Ju, H. (2010) Fluorescence resonance energy transfer between quantum dots and graphene oxide for sensing biomolecules. *Anal. Chem. 82*, 5511−5517.
(12) Derfus, A. M., Chan, W. C. W., and Bhatia, S. N. (2004) Probing the cytotoxicity of semiconductor quantum dots. *Nano Lett. 4*, 11−18.
(13) Yang, P., and Murase, N. (2010) Preparation-condition dependence of hybrid SiO_2-coated CdTe nanocrystals with intense and tunable photoluminescence. *Adv. Funct. Mater. 20*, 1258−1265.
(14) Murase, N., and Yazawa, T. (2001) Partially reduced cuprous oxide nanoparticles formed in porous glass reaction fields. *J. Am. Ceram. Soc. 84*, 2269−2273.
(15) Jiang, Y. Y., Liu, C., Hong, M. H., Zhu, S. J., and Pei, Y. Y. (2007) Tumor cell targeting of transferrin-PEG-TNF-α conjugate via a receptor-mediated delivery system: design, synthesis, and biological evaluation. *Bioconjugate Chem. 18*, 41−49.
(16) Huang, R. K., Steinmetz, N. F., Fu, C. Y., Manchester, M., and Johnson, J. E. (2010) Transferrin-mediated targeting of bacteriophage HK97 nanoparticles into tumor cells. *Nanomedicine 6*, 55−68.
(17) Hummers, W. S., and Offeman, R. E. (1958) Preparation of graphitic oxide. *J. Am. Chem. Soc. 80*, 1339−1339.
(18) Yang, X., Zhang, X., Ma, Y., Huang, Y., Wanga, Y., and Chen, Y. (2009) Superparamagnetic graphene oxide-Fe_3O_4 nanoparticles hybrid for controlled targeted drug carriers. *J. Mater. Chem. 19*, 2710−2714.
(19) Al-Jamal, W. T., Al-Jamal, K. T., Tian, B., Cakebread, A., Halket, J. M., and Kostarelos, K. (2009) Tumor targeting of functionalized quantum dot-liposome hybrids by intravenous administration. *Mol. Pharmaceutics 6*, 520−530.
(20) Laemmli, U. K. (1970) Cleavage of structural proteins during assembly of head of bacteriophage-T4. *Nature 227*, 680−685.
(21) Chen, M. L., Chen, M. L., Chen, X. W., and Wang, J. H. (2010) Functionalization of MWNTs with hyperbranched PEI for highly selective isolation of BSA. *Macromol. Biosci. 10*, 906−915.
(22) Ferrari, A. C., Meyer, J. C., Scardaci, V., Casiraghi, C., Lazzeri, M., Mauri, F., Piscanec, S., Jiang, D., Novoselov, K. S., Roth, S., and Geim, A. K. (2006) Raman spectrum of graphene and graphene layers. *Phys. Rev. Lett. 97*, 187401−4.
(23) Zhu, Y., Murali, S., Cai, W., Li, X., Suk, J. W., Potts, J. R., and Ruoff, R. S. (2010) Graphene and graphene oxide: synthesis, properties, and applications. *Adv. Mater. 22*, 3906−3924.
(24) Li, D., Muller, M. B., Gilje, S., Kaner, R. B., and Wallace, G. G. (2008) Processable aqueous dispersions of graphene nanosheets. *Nat. Nanotechnol. 3*, 101−105.
(25) Zhang, X., Meng, L., Lu, Q., Fei, Z., and Dyson, P. J. (2009) Targeted delivery and controlled release of doxorubicin to cancer cells using modified single wall carbon nanotubes. *Biomaterials 30*, 6041−6047.
(26) Shimizu, K. T., Woo, W. K., Fisher, B. R., Eisler, H. J., and Bawendi, M. G. (2002) Surface-Enhanced Emission from Single Semiconductor Nanocrystals. *Phys. Rev. Lett. 89*, 117401(1−4).
(27) Fan, H. M., Olivo, M., Shuter, B., Yi, J. B., Bhuvaneswari, R., Tan, H. R., Xing, G. C., Ng, C. T., Liu, L., Lucky, S. S., Bay, B. H., and Ding, J. (2010) Quantum dot capped magnetite nanorings as high performance nanoprobe for multiphoto fluorescence and magnetic resonance imaging. *J. Am. Chem. Soc. 132*, 14803−14811.
(28) Pawar, L. S., Badhwar, A., Kharas, F., Khandare, Jayant., and Vavia, P. R. (2012) Design, synthesis and evaluation of N-acetyl glucosamine (NAG)-PEG doxorubicin targeted conjugates for anticancer delivery. *Int. J. Pharmaceut. 436*, 183−193.
(29) Zhang, L., Xia, J., Zhao, Q., Liu, L., and Zhang, Z. (2010) Functional graphene oxide as a nanocarrier for controlled loading and targeted delivery of mixed anticancer drugs. *Small 6*, 537−544.
(30) Chen, F. H., Zhang, L. M., Chen, Q. T., Zhang, Y., and Zhang, Z. J. (2010) Synthesis of a novel magnetic drug delivery system composed of doxorubicin-conjugated Fe_3O_4 nanoparticle cores and a PEG-functionalized porous silica shellw. *Chem. Commun. 46*, 8633−8635.
(31) Zhu, Y., Murali, S., Cai, W., Li, X., Suk, J. W., Potts, J. R., and Ruoff, R. S. (2010) Graphene and graphene oxide: synthesis, properties, and applications. *Adv. Mater. 22*, 3906−3924.
(32) Li, D., Muller, M. B., Gilje, S., Kaner, R. B., and Wallace, G. G. (2008) Processable aqueous dispersions of graphene nanosheets. *Nat. Nanotechnol. 3*, 101−105.
(33) Liu, Z., Sun, X., Ratchford, N. N., and Dai, H. (2007) Supramolecular chemistry on water- soluble carbon nanotubes for drug loading and delivery. *ACS Nano 1*, 50−56.
(34) Setua, S., Menon, D., Asok, A., Nair, S., and Koyakutty, M. (2010) Folate receptor targeted, rare-earth oxide nanocrystals for bi-modal fluorescence and magnetic imaging of cancer cells. *Biomaterials 31*, 714−729.
(35) Kim, J., Lee, J. E., Lee, S. H., Yu, J. H., Lee, J. H., Park, T. G., and Hyeon, T. (2008) Designed fabrication of a multifunctional polymer nanomedical platform for simultaneous cancer-targeted imaging and magnetically guided drug delivery. *Adv. Mater. 20*, 478−483.